



Disruption of mitochondrial function augments the radiosensitivity of prostate cancer cell lines

Grzegorz Michał Adamczuk^{1,2,A-D,F}✉, Ewelina Humeniuk^{1,2,B-C}, Kamila Adamczuk^{1,3,C-D},
Barbara Madej-Czerwonka^{1,4,D}, Jarosław Dudka^{1,5,A}

¹ Medical University, Lublin, Poland

² Independent Medical Biology Unit, Lublin, Poland

³ Department of Biochemistry and Molecular Biology, Medical University, Lublin, Poland

⁴ Human Anatomy Department, Medical University, Lublin, Poland

⁵ Department of Toxicology, Medical University, Lublin, Poland

A – Research concept and design, B – Collection and/or assembly of data, C – Data analysis and interpretation, D – Writing the article, E – Critical revision of the article, F – Final approval of the article

Adamczuk GM, Humeniuk E, Adamczuk K, Madej-Czerwonka B, Dudka J. Disruption of mitochondrial function augments the radiosensitivity of prostate cancer cell lines. *Ann Agric Environ Med.* 2023; 30(1): 65–76. doi: 10.26444/aaem/155382

Abstract

Introduction. Ionizing radiation is one of the most widely used therapeutic methods in the treatment of prostate cancer, but the problem is developing radioresistance of the tumour. There is evidence that metabolic reprogramming in cancer is one of the major contributors to radioresistance and mitochondria play a crucial role in this process.

Objective. The aim of the study was to assess the influence of oxidative phosphorylation uncoupling to radiosensitivity of prostate cancer cells differing in metabolic phenotype.

Materials and method. LNCaP, PC-3 and DU-145 cells were exposed to X-rays and simultaneously treated with 2,4-dinitrophenol (2,4-DNP). The radiosensitivity of cell lines was determined by cell clonogenic assay and cell cycle analysis. The cytotoxic effect was evaluated with MTT and CVS (Crystal violet staining) assay, apoptosis detection and cell cycle analysis. The phenotype of the cells was determined by glucose uptake and lactate release, ATP level measurement as well as basal reactive oxygen species level and mRNA expression of genes related to oxidative stress defence.

Results. The synergistic effect of 2,4-dinitrophenol and X-ray was observed only in the case of the LNCaP cell line.

Conclusions. Phenotypic analysis indicates that this may be due to the highest dependence of these cells on oxidative phosphorylation and sensitivity to disruption of their redox status.

Key words

prostate cancer, X-ray, mitochondria, radiosensitivity, metabolic phenotype, dinitrophenol

INTRODUCTION

Despite significant advances in medicine, neoplastic diseases are the second leading cause of death worldwide [1]. Prostate cancer in world statistics ranks high in terms of both morbidity and mortality [2]. Currently, radiotherapy is a radical treatment option for patients with localized prostate cancer, but it can also become one of the adjuvant treatment options [3]. The effectiveness of radiotherapy is influenced by many factors, such as the radiosensitivity of the tumour cells.

The mechanism of X-ray action can be both direct and indirect. X-rays directly interact with the atoms of the DNA molecule as a result of the shield effect. The indirect effect of DNA damage is mainly caused by free radicals (such as hydroxyl radical- OH[•] and superoxide radical- HO₂[•]) resulting from the radiolysis of water present in the cells [4, 5]. In addition, X-rays can disrupt the function of the cell membrane and intracellular organelles through, e.g. oxidative damage not only to DNA but also to lipids and proteins, and they may also change the activity of DNA damage response signalling pathways to control cancer cell cycle arrest and cell viability [4–7]. Due to the increasing radioresistance of cancer cells, radiotherapy often becomes an ineffective method in

therapy. The resistance to radiotherapy in neoplastic cells is associated with changes in the metabolic phenotype of the tumour [8, 9].

The most common change in cellular metabolism is the Warburg effect, characterized by the preference of cancer cells to generate energy via the glycolytic pathway despite the presence of oxygen. The aforementioned effect leads to tumour progression by activation of oncogenes as phosphatidylinositol 3-kinase (PI3K) and hypoxia inducible factor-1 alpha (HIF-1A) which cause change of tumour microenvironment [10, 11]. At first, it was postulated that this effect originated from dysfunctional mitochondria in tumour cells. Nowadays, however, it is known that the majority of cancer cells possess functional mitochondria and willingly use both aerobic glycolysis and OXPHOS (Oxidative phosphorylation) to support the production of ATP, oxidative stress regulators (such as NADPH and GSH), macromolecules and oncometabolites, depending on the tumour microenvironment, oxygen and nutritious supply, as well as stage of disease [12, 13]. A growing body of evidence demonstrates that changes in mitochondrial function and metabolism have an impact on cancer progression and treatment effectiveness through the regulation of mitochondrial energy production [14]. Many genes and signalling pathways are involved in this process, i.e. through PI3K/AKT and p53 pathways [15, 16].

The study of the processes underlying the development of cancer resistance to radiation therapy is another chance for

✉ Address for correspondence: Grzegorz Michał Adamczuk, Medical University, Lublin, Poland
E-mail: grzegorzadamczuk@umlub.pl

Received: 18.07.2022; accepted: 13.10.2022; first published: 21.10.2022

the emergence of new therapeutic strategies based on the sensitization of cancer cells to radiation. Due to the essential role of mitochondria in metabolism and cell survival, targeting mitochondria in cancer cells is an attractive therapeutic strategy.

In the present study, 2,4-dinitrophenol (2,4-DNP) was used as a potential radiosensitizer, due to evidences about its ability to induce oxidative stress and disrupt ATP production in cancer cells. 2,4-DNP is an organic compound originally used in the treatment of obesity. It accelerates the basal metabolism of obese people by burning more carbohydrates and fat, which results in weight loss. 2,4-DNP reduces ATP production in the mitochondria (Fig. 1). This is possible due to the uncoupling of oxidative phosphorylation. Changes in the potential of the mitochondrial membrane cause the resulting energy to be dissipated in the form of heat, bypassing the ATP synthesis stage [17, 18].

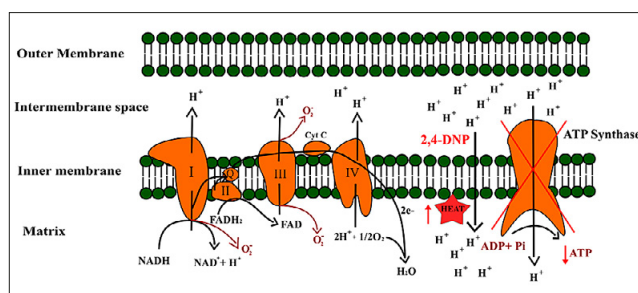


Figure 1. Graphical presentation of decreased ATP production due to uncoupling of oxidative phosphorylation by 2,4-dinitrophenol in the mitochondria

OBJECTIVE

The aim of the study was to sensitize prostate cancer cells to X-rays, as well as to enhance its effectiveness using 2,4-DNP as an uncoupler. It was chosen due to the fact that 2,4-DNP is a well-known and thoroughly researched model uncoupler substance. In the study, an attempt was made to correlate obtained results with the metabolic phenotype of prostate cancer cell lines. The assumption of the study was to present a possible new therapeutic strategy depending on the metabolic phenotype of prostate cancer cells based on the disruption of mitochondrial function by the uncoupler.

MATERIALS AND METHOD

Cell culture and treatment. Three metastatic prostate cancer cell lines (PC-3, DU-145- hormone-insensitive, LNCaP-hormone-sensitive) and embryonic rat cardiomyocytes (H9c2(2-1)) were used in the study (ATCC, USA). PC-3 cells were cultured in Kaighn's Modification of Ham's F-12 Medium (F12-K) (ATCC, USA), DU-145 cells in Eagle's Minimum Essential Medium (EMEM) (ATCC, USA), LNCaP cells in RPMI-1640 Medium (ATCC, USA) and H9c2(2-1) cells in Dulbecco's Modified Eagle Medium (DMEM) (ATCC, USA). All experiments were performed on cell lines to 15 passages due to the fact that prolonged passaging change phenotype as well as genotype of cancer cells. The media were supplemented with 10% fetal bovine serum (Corning, USA) and cells incubated at 37°C with 5% CO₂ in an air atmosphere. During culturing, all cell lines were tested for

mycoplasma contaminations using Venor®GeM OneStep-Mycoplasma Detection Kit (Minerva Biolabs, Germany). The tested cells were incubated for 48 h with 2,4-DNP (Sigma-Aldrich, Switzerland) in following concentrations: 5, 10, 50, 100, 250, 500, 1,000 μM and exposed to X-rays in doses: 1, 2.5, 5, 10 Gy.

This preliminary study was necessary to select the optimal 2,4-DNP concentration and X-ray dose. In further studies, the cells were incubated for 48 h after being exposed for 5 Gy doses of X-ray and 100 μM 2,4-DNP.

Exposure to X-rays. The cells were exposed to X-rays in increasing doses of radiation. The X-rays doses used for the research were selected on the basis of the available scientific data and are in line with the doses used in the clinic, e.g. conventionally fractionated external-beam radiation therapy (1.8–2.0 Gy/fraction) and accelerated hypofractionation (5–10 Gy/fraction). The irradiation of the cells was performed using the radiator of the biological material RS-2000 Biological Irradiator (Rad Source Technologies, USA). The radiation doses were obtained at the intensity of 25 mA, voltage of 160 kV and the appropriate irradiation time (4 Gy/min). Cells in the control group not treated with X-rays were incubated keeping the same incubation time as tested cells groups.

MTT Assay. To determine the cytotoxicity of 2,4-DNP with/without X-ray radiation on prostate cancer cell lines, the MTT assay was performed. The MTT test is based on the reduction of the orange tetrazolium salt to water-insoluble purple formazan crystals by succinate dehydrogenase observed in living cells. In all assays, the cells were seeded in the concentration of 1.5×10^5 cells/mL. 2,4-DNP was added when 70–80% of the confluence of cells was achieved. In the case of simultaneously testing the effect of 2,4-DNP with X-ray, the cells were exposed to 5 Gy after 1 h incubation with 100 μM 2,4-DNP. After 48 h incubation of cells, a freshly-prepared MTT solution (0.5 mg/mL in phosphate-buffered saline) was added. After 3 hours of incubation with MTT solution, the medium was removed and the formazan crystals were dissolved in DMSO. The absorbance of the obtained solutions was measured at 570 nm with a PowerWave XS microplate spectrophotometer (BioTek Instruments, USA). Hence, the absorbance level corresponds with the observed amount of formazan and is proportional to the number of living cells. Each assay was conducted 3 times and measured in triplicates. The IC₅₀ value for 2,4-DNP was determined using the AAT Bioquest IC₅₀ calculator [19].

CVS Assay. To determine the cytotoxicity of 2,4-DNP on prostate cancer cell lines, CVS assay was also performed. The CVS test was performed due to reports of possible inhibition of succinate dehydrogenase (the enzyme on which the MTT test is based) by 2,4-DNP. Crystal violet stains the cells as a result of DNA and proteins binding. This assay is based on staining attached cells to the surface of the plate. The stained dead cells were detached from the plate surface and thus washed away. After 48 h incubation with the tested compound, the medium was removed and the cells were rinsed with PBS. Then, 50 μl of a 0.5% solution of crystal violet (dissolved in distilled water and methanol in the ratio of 4:1) was added. After 20 min of incubation, the solution was removed and cells rinsed 3 times with PBS. When the plate had dried, the 200 μl of methanol was added to dissolve

the remaining dye. The absorbance of the obtained solutions was measured at 595 nm with a PowerWave XS microplate spectrophotometer (BioTek Instruments, USA). Hence, the absorbance level correlates with the observed amount of remaining dye and is proportional to the number of living cells. Each assay was conducted 3 times and measured in triplicate.

Cell cycle analysis. The cell cycle was studied using NucleoCounter NC-3000 (ChemoMetec, Allerød, Denmark) according to the 2-step Cell Cycle Assay protocol (ChemoMetec, Allerød, Denmark). After incubation, the cells were detached from the plate using trypsin, suspended in 250 µl lysis buffer (Solution 10) enriched with 10 µg/mL DAPI (4',6-Diamidine-2'-phenylindole dihydrochloride) and incubated for 5 min at 37 °C in the dark. Then, 250 µl of stabilization buffer (Solution 11) was added. The obtained cells suspension was applied onto the NC-Slide and analyzed in NucleoCounter NC-3000. Each experiment was conducted 3 times with measurements in triplicate.

Clonogenic assay. The radiosensitivity of the prostate cancer cell lines was determined by clonogenic assay. After 24 h of exposition to X-ray in a wide range of doses (1–10 Gy), the cells were trypsinized and counted. Then, 2×10^3 (PC-3, DU-145) and 4×10^3 (LNCaP) cells were seeded to 6-well plates and incubated for a 5-doubling time. After incubation, the formed colonies were fixed and stained with 0.5% crystal violet. The absorbance of extracted dye was measured at 595 nm with a PowerWave XS microplate spectrophotometer (BioTek Instruments, USA). This indicates the clonogenic potential of prostate cancer cell cultures. Each experiment was conducted 3 times with measurement in triplicate.

Assessment of cells morphology. Cell morphology was assessed using a phase-contrast microscope Nikon Eclipse Ti and NIS-Elements Imaging Software (Nikon, Tokyo, Japan).

Detection of apoptosis. Apoptosis detection was studied using NucleoCounter NC-3000 (ChemoMetec, Allerød, Denmark) according to the Annexin V Apoptosis Assay (ChemoMetec, Allerød, Denmark). After 48 h of incubation, the cells were detached from the plate using trypsin-EDTA solution (Corning, Corning, USA). Then, cells were centrifugated at 400 g for 5 minutes, and resuspended in PBS. Next, centrifugated cells were stained with the Annexin V-FITC, Hoechst 33342 and PI, according to the manufacturer's recommended protocol. The stained cells were applied into the NC-Slide and analyzed in NucleoCounter NC-3000. Each experiment was conducted three times with measurement in triplicate.

ATP level measurement. The ATP level was measured using ATP Colorimetric/Fluorometric Assay Kit (Sigma-Aldrich). The cells were treated with 2,4-DNP (100 µM) for 48 h and then they were moved out and counted with Countess Automated Cell Counter (Invitrogen, USA). Simultaneously, the cells incubated without 2,4-DNP were used as a control in the performed experiment. Subsequently, 2×10^6 cells were suspended in a 20 µl ATP Assay Buffer. The cells solution was filtrated by means of a 10 kDa Molecular Weight Cut off (MWCO) column to deproteinate the samples and obtained filtrate was used for further analysis. The assay was performed in a 96-well flat-bottom culture plate. 50 µl of the reaction

mixture was applied to the wells, which consisted of: ATP Assay Buffer 44 µl, ATP Probe 2 µl, ATP Converter 2 µl, Developer Mix 2 µl. Then, 30 µl of the obtained filtrates were added to the reaction wells and filled to 100 µl with the ATP Assay Buffer. The plate was placed on a shaker and incubated for 30 minutes at room temperature. After incubation, the absorbance of the samples was measured at 570 nm with a PowerWave XS microplate spectrophotometer (BioTek Instruments, USA).

Glucose and lactate measurement. To assess the metabolic phenotype of tested prostate cancer cell lines, the concentrations of lactate and glucose were measured after 24 h and 48 h of cells incubation. Glucose concentration in the culture media was measured using the GlucCell® GLUCOSE MONITORING SYSTEM (CESCO Bioengineering, Taiwan) and disposable test strips. The lactate concentration in media was measured using the Lactate Plus Meter (Nova Biomedical, Waltham, USA) with the use of dedicated strips. The concentration of consumed glucose and synthesized lactate were normalized to the sample protein concentration.

Quantitative Real-Time PCR Analysis (qRT-PCR). The cells of the 3 cell lines were seeded into a 6-well plate. To lyse the cells the TRIzol Reagent (Invitrogen, Carlsbad, USA) was added when 70–80% of confluency was achieved. Next, RNA was isolated according to the Chomczynski and Sacchi method. Isolated RNA was reverse transcribed with an NG dART RT-PCR kit (EURx, Gdańsk, Poland) according to the manufacturer's instructions. The qPCR was conducted using PowerUp SYBR Green Master Mix (ThermoFisher, Waltham, USA) according to the manufacturer's instructions in a 7500 Fast Real-Time PCR System (ThermoFisher, USA). The reaction was carried out in triplicate. The relative expression of tested genes was determined by qRT-PCR and the $\Delta\Delta C_t$ method using *18S RNA* and *BACT* as reference genes. Statistical analysis was performed with RQ values (relative quantification, $RQ = 2^{-\Delta\Delta C_t}$). The primer sequences were summarized in Table 1.

Table 1. qPCR primers used in the experiment

Target (Abbreviation)	Forward	Reverse
Glutathione peroxidase 1 (<i>GPX1</i>)	TTGACATCGAGCCTGACATC	ACTGGGATCAACAGGACCAG
Glutathione-disulfide reductase (<i>GSR</i>)	TCAGCTACCACAACCTCTG	GAGACCAGCCTGACCAACAT
Superoxide dismutase 2 (<i>SOD2</i>)	CTTCAGGGTGGTATGGCTGT	TGGCCAGACCTTAATGTCC
Catalase (<i>CAT</i>)	AGCTTAGCGTTCATCCGTGT	TCCAATCATCCGTCAAACA
18S Ribosomal RNA (<i>18S RNA</i>)	GAAACTGCGAATGGCTCATTAAACACAGTATCCAAGTGGGAGAGG	
B-Actin (<i>BACT</i>)	AGAGCTACGAGCTGCCTGAC	AGCACTGTGTGGCGTACAG

Reactive oxygen species (ROS) detection. The CellROX Green Reagent (Invitrogen, USA) was used for ROS detection.

The CellROX acts as a fluorogenic probe that is weakly fluorescent while in a reduced state. It exhibits bright green photostable fluorescence upon oxidation by ROS.

The cells were seeded into 6-well plates. The cells were stained with 5 μ M CellROX[®] Orange Reagent when 70–80% of confluence was achieved. After incubating at 37°C for 30 min. the cells were washed twice with PBS and imaged on a Nikon Eclipse Ti inverted microscope using a 20X objective with NIS-Elements Imaging Software (Nikon, Tokyo, Japan).

Statistical analysis. The data were analysed using the STATISTICA vs. 13 application (StatSoft, Poland). The results were expressed as mean \pm standard deviation (SD). For comparison of more than 2 groups of means, the one-way analysis of variance (ANOVA) and *post hoc* multiple comparisons on a basis of Tukey's HSD test were used. All parameters were considered statistically significantly different if *p* values were less than 0.05.

RESULTS

Cytotoxic analysis

X-ray. To select the appropriate dose of ionising radiation for further studies, an analysis of the cell cycle cells was carried out 24 h after irradiation. Additionally, the radiosensitivity of tested prostate cancer cell lines was tested using a clonogenic assay. Cell cycle analysis of cells showed an increased % of cells in the G2 phase with increasing radiation dose (Fig. 2A-C). These changes were best observed when the highest doses of 5 Gy were used. In the clonogenic assay, the LNCaP was the most radiosensitive cell line compared to others tested (Fig. 2D-E). Only the exposure of 3 cell lines to 5 Gy contributed to the decrease in absorbance below 50% compared to the control. For the reasons mentioned above, the dose of 5 Gy was selected for further studies.

2,4-DNP. The MTT assay and the CVS test were used to evaluate the cytotoxicity of 2,4-DNP. The MTT assay is based

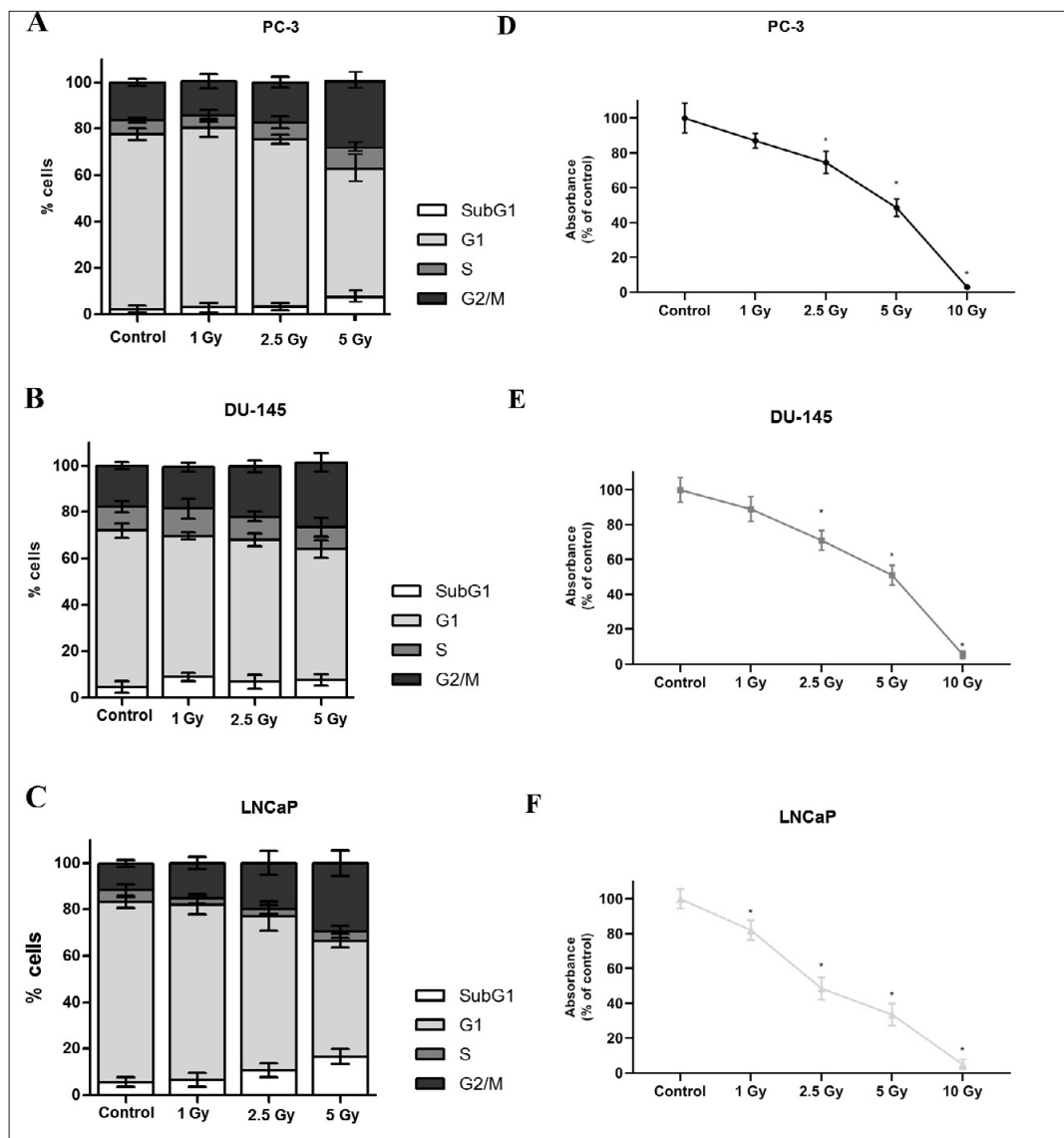


Figure 2 (A-C). Cell cycle analysis by image cytometry. The prostate cancer cells were exposed to X-ray in a wide range of doses (1–5 Gy) and incubated for 24 h. The values obtained from 3 independent experiments were presented as mean \pm SD. **(D-E)** Dose-response curves of prostate cancer cell lines exposed to X-ray in a wide range of doses (1–10 Gy) by clonogenic assay. The values obtained from 3 independent experiments were presented as mean \pm SD.

* *p* < 0.05 vs. control.

on the ability to metabolize a tetrazolium salt to formazan crystals by succinate dehydrogenase active only in living cells. Crystal violet used in CVS assay, stains live and attached to the plate cells as a result of DNA and protein binding. It is a non-enzymatic assay as compared to the MTT test.

The MTT assay confirmed the toxicity of 2,4-DNP against 3 prostate cancer cell lines (Fig. 3A). Prostate cancer cell lines were treated with 2,4-DNP in a wide concentration range of 5–1,000 μM . The use of at least 50 μM 2,4-DNP caused a statistically significant decrease in cells viability. Additionally, a gradual decrease in cell viability was observed with the increasing concentration of the compound used. The concentration of 100 μM of 2,4-DNP was in the range of IC_{60-80} for the tested cell lines; therefore, this concentration of the compound was selected for further studies. The selected concentration was below the concentration range determined in biological fluids of patients presenting symptoms of poisoning [17, 20].

The H9c2(2–1) was used as a normal cell line to test 2,4-DNP toxicity. The cardiomyocytes preferentially use oxidative phosphorylation for energy generation. It has been found that H9c2(2–1) cells were close to normal primary cardiomyocytes concerning their energy metabolism features [18, 19, 21, 22]. Thus, it was speculated that the H9c2(2–1) cell line should be the most sensitive for uncoupler treatment. The selected concentration of 2,4-DNP (100 μM) was not cytotoxic to H9c2(2–1) cardiac myoblasts (Fig. 3B). 2,4-DNP significant decrease viability of cells in the concentration of 500 μM and higher was observed compared to control.

The CVS test was performed on the basis of reports concerning the possible inhibition of succinate dehydrogenase by 2,4-DNP. The reliability of the MTT test in relation to 2,4-DNP was confirmed by the CVS test on one of the selected prostate cancer cell lines – PC-3. The results obtained in the CVS test are highly comparable to the results obtained in the MTT test (Fig. 3C).

2,4-DNP and X-ray

MTT. The MTT test showed a statistically significant decrease in the viability of LNCaP prostate cancer cells treated simultaneously with 100 μM 2,4-DNP and 5 Gy X-rays, compared to the cells treated with the mentioned factors separately (Fig. 4). In this case, LNCaP cells viability decreased below 20%. The synergistic effect of 2,4-DNP with ionizing radiation occurred only on the LNCaP cell line. On the other hand, in the case of the PC-3 and DU-145 prostate cancer lines, no statistically significant decrease was observed in cell viability in relation to the 2,4-DNP used alone.

Cell cycle analysis. In the case of simultaneous incubation of prostate cancer cells of the PC-3 cell line and DU-145 cell line with 2,4-DNP at a concentration of 100 μM and exposure to X-rays at a dose of 5 Gy, an increased cytostatic effect of X-rays was observed (Fig. 5). Analysis of the cell cycle showed more cells arrested in the G2 cell cycle phase, compared to the cells treated with X-rays alone. 2,4-DNP used alone has no effect on the cell cycle. The obtained results were similar to the control sample.

The cell cycle analysis of LNCaP cells treated with 2,4-DNP indicates the presence of the cytotoxic effect of the tested compound via an increase in the population of cells in the subG1 phase, corresponding to dead cells and also a decrease in the population of cells in the G1 phase, compared to control cells (Fig. 5). The cells exposed to 5 Gy showed

the cytotoxic effect of X-ray as well as a cytostatic effect by observed increases sub G1 phase and G2 phase of the cell cycle, respectively. Analysis of the cell cycle of cells treated simultaneously with X-ray and 2,4-DNP showed a big decrease in the G2 phase, a sharp increase in the subG1 phase in relation to LNCaP cells treated with X-ray alone, as well as an increase in the subG1 phase, compared to the sample treated with 2,4-DNP alone. The demonstrated changes in the cell cycle indicate its strong cytotoxic effect caused by the addition of 2,4-DNP.

Assessment of Cells Morphology. The results obtained from the MTT test and cell cycle analysis are consistent with the cell morphology assessment (Fig. 6). The control PC-3, DU-145 and LNCaP cells represented typical epithelial-like morphology.

The number of cells observed in the field of view was decreased after treatment of both PC-3 and DU-145 cells with 2,4-DNP and X-ray alone. (Fig. 6 A,B). Furthermore, simultaneous treatment of PC-3 and DU-145 cells with 2,4-DNP and X-ray resulted in a visibly decreased number of cells, compared to control. In PC-3 culture treated simultaneously with X-ray and 2,4-DNP, the cells were similar to the cells treated with 2,4-DNP alone, whereas cells exposed to 5 Gy alone did not differ from control cells. In the case of DU-145 cells, treatment with 2,4-DNP alone as well as simultaneous treatment with 2,4-DNP and X-ray, resulted in morphological changes such as shrinkage and rounding of cells and their loss of attachment ability.

On the contrary, treatment of LNCaP cells with 2,4-DNP or X-rays resulted in the most significant changes in cells morphology (Fig. 6C). LNCaP cells exposed to 5 Gy became more stellate-like morphologically and spindle-shaped. Incubation with 2,4-DNP caused the cells to become more shrunken. In both cases, the number of cells was visibly reduced. Simultaneous treatment of the LNCaP cells with 2,4-DNP and X-ray resulted in intensification of the mentioned morphological changes. Numerous cells observed in the field of view were shrunken, dead and detached.

Detection of apoptosis. Analysis of apoptosis revealed that cells treated with 2,4-DNP were clearly in the early stage of apoptosis (Fig. 7). After X-ray exposition, the cells were both early- and late- apoptotic. In the histogram, which represented simultaneous treated LNCaP cells with 2,4-DNP and 5 Gy of X-ray, the percentage of cells in the late stage of apoptosis increased (almost all cells were in the late stage of apoptosis/late apoptotic).

Metabolic phenotype of prostate cancer cell lines

ATP concentration measurement. This test was used to assess the dependence of the tested cells on oxidative phosphorylation through the ability of 2,4-DNP to inhibit ATP synthesis.

The highest decrease (over 60 ng/ μL compared to control) of ATP concentration was observed for the LNCaP cell line (Fig. 8). In addition, the LNCaP cell line was characterized by the highest basal ATP concentration (almost 2-fold higher), compared to the other 2 tested prostate cancer cell lines. Treatment with 2,4-DNP decreased the ATP concentration in PC-3 and DU-145 cell lines by about 10 and 15 ng/ μL , respectively. Therefore, the LNCaP cell line was shown to be the most dependent on oxidative phosphorylation as compared to others.

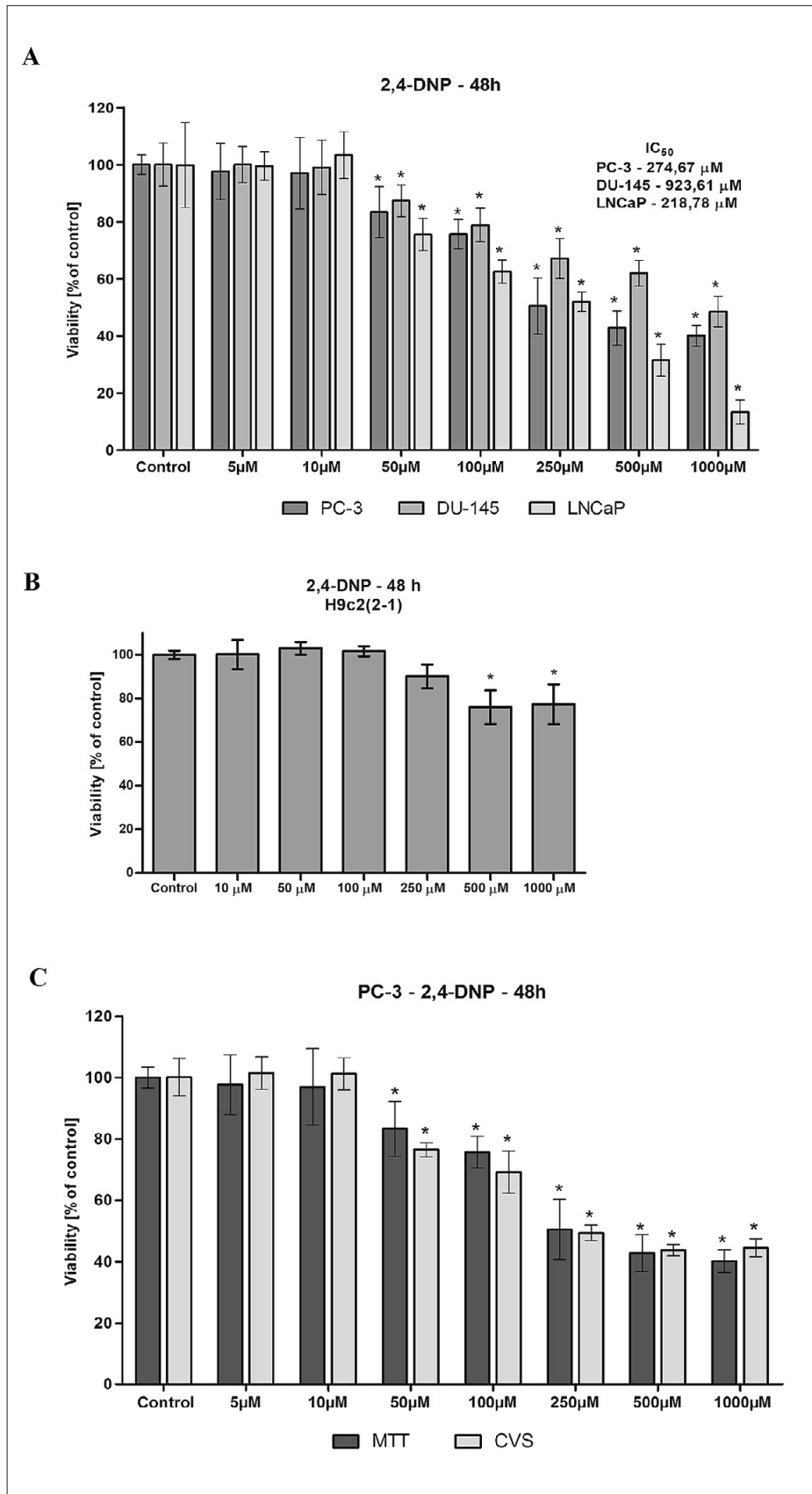


Figure 3. (A) Prostate cancer cell lines (PC-3, DU-145, LNCaP) and (B) Cardiomyoblast cell line (H9c2(2-1)) viability (% of control) based on MTT assay. The cells were treated with a wide range of 2,4-DNP concentrations for 48 h. The values obtained from 3 independent experiments were presented as mean \pm SD. * $p < 0.05$ vs. control. (C) The PC-3 cell viability (% of control) based on MTT test compared to CVS assay. The cells were treated with a wide range of 2,4-DNP concentrations (5–1000 μ M) for 48h. The values obtained from 3 independent experiments were presented as mean \pm SD. * $p < 0.05$ vs. control

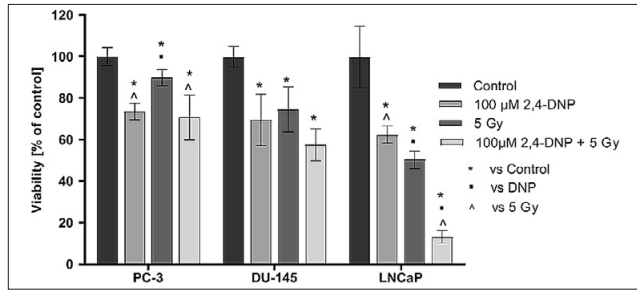


Figure 4. Prostate cancer cell lines (PC-3, DU-145, LNCaP) viability (% of control) based on MTT assay. The cells were treated with 100 μM of 2,4-DNP and exposed to 5 Gy of X-ray or combined (2,4-DNP + X-ray) for 48 h. The values obtained from 3 independent experiments were presented as mean ±SD. * p<0.05 vs. control, ^ p< vs. DNP, Δ p<0.05 vs. 5 Gy

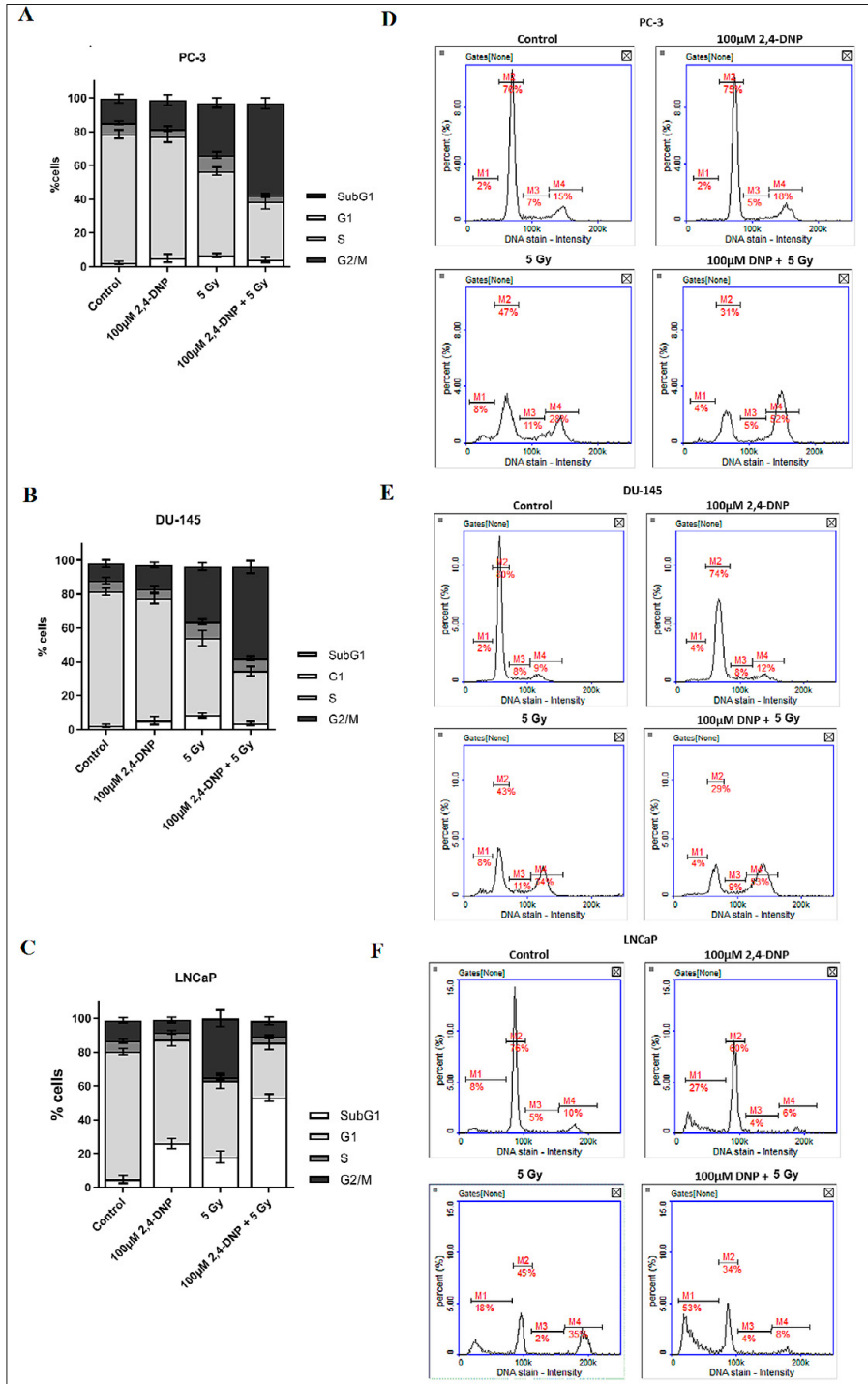


Figure 5 (A-C) Cell cycle analysis by image cytometry. The prostate cancer cells were treated with 100 μM of 2,4-DNP for 48 h and exposed to 5 Gy of X-ray or combined (2,4-DNP + X-ray). The values obtained from 3 independent experiments were presented as mean ±SD. **(D-F)** Histograms representative of all repetitions of the experiment (M1- subG1, M2- G1, M3- S, M4- G2/M phase).

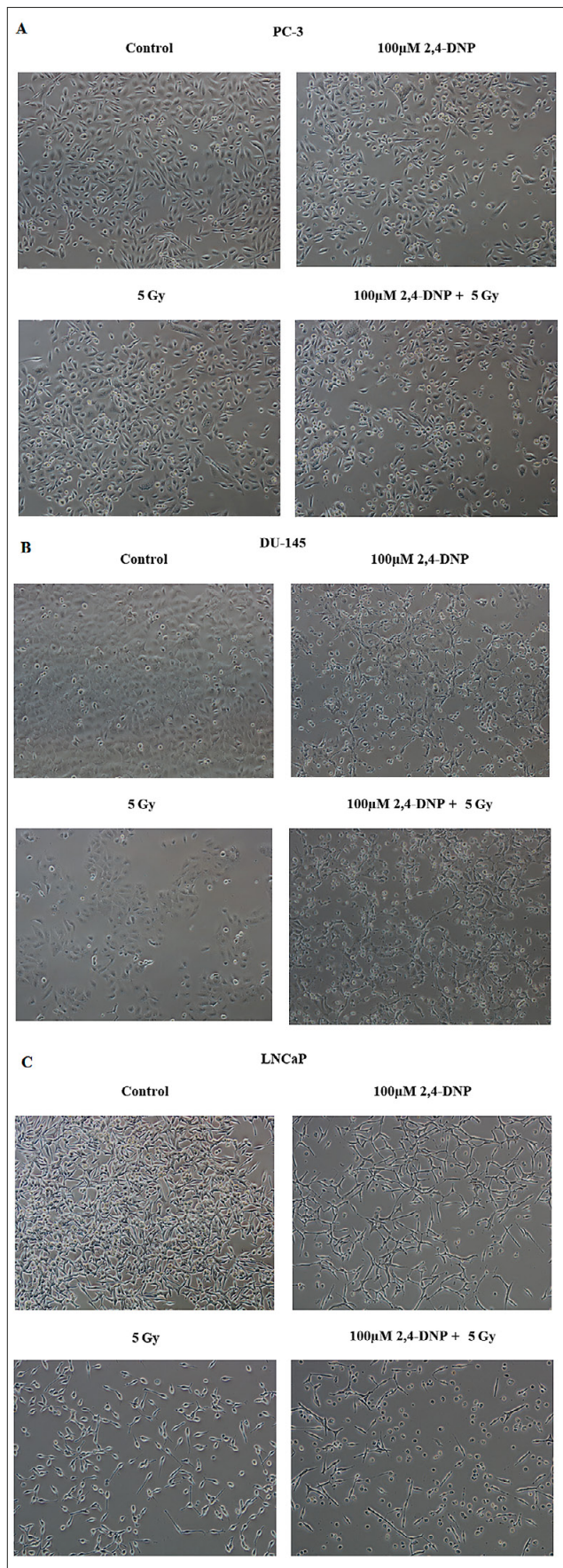


Figure 6. Morphological changes of **A**) PC-3, **B**) DU-145 and **C**) LNCaP cells. The cells were treated for 48 h with 100 μM 2,4-DNP and 5 Gy of X-ray or combined (magnification x 100)

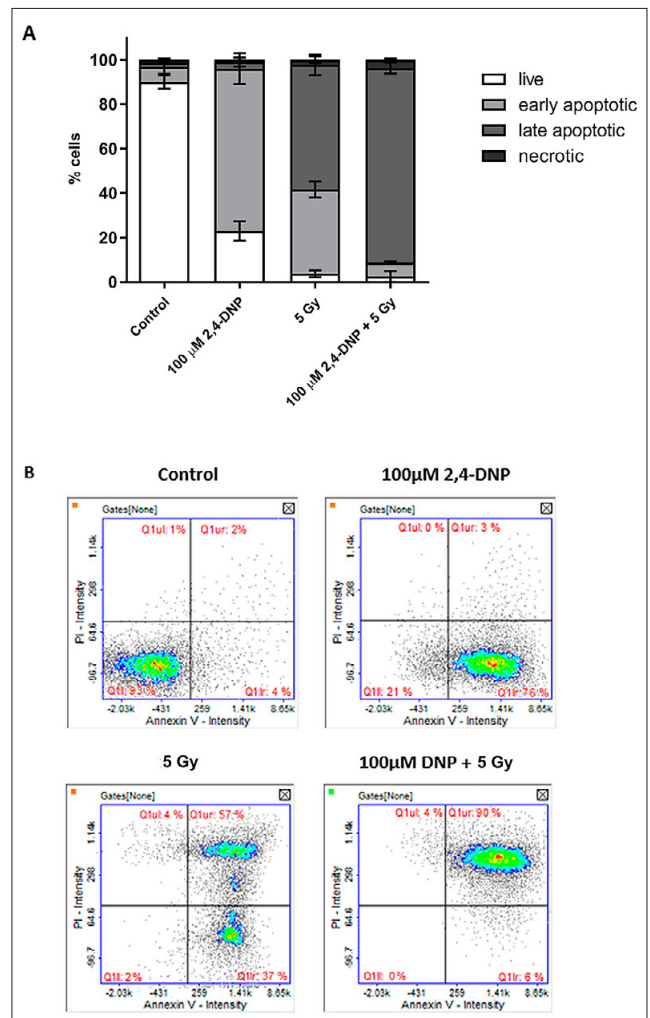


Figure 7 (A) Detection of apoptosis analysis by image cytometry. The LNCaP cells were treated with 100 μM of 2,4-DNP and exposed to 5 Gy of X-ray or combined (2,4-DNP + X-ray) for 48 h. The values obtained from 3 independent experiments were presented as mean ±SD. **B**) Histograms representative for all repetitions of the experiment (Q1I- live, Q1I- early apoptotic, Q1I- late apoptotic and Q1I- necrotic cells)

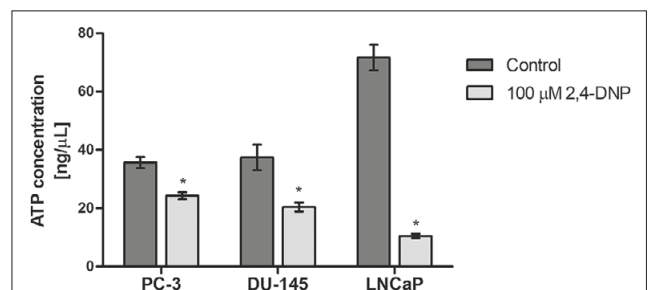


Figure 8. Changes of ATP concentration after 48 h incubation of prostate cancer cell lines with 2,4-DNP at 100 μM concentration

Glucose and lactate measurement. The measurement of glucose and lactate concentrations in culture media revealed that LNCaP cells during their 48 h culturing consumed the least glucose and produced the least lactate, compared to other prostate cancer cell lines (Fig. 9). In the case of PC-3, after 48 h culturing, cells consumed a lower amount of glucose compared to DU-145, but at the same time produced the highest amount of lactate. DU-145 cells, on the other hand, consumed the most glucose.

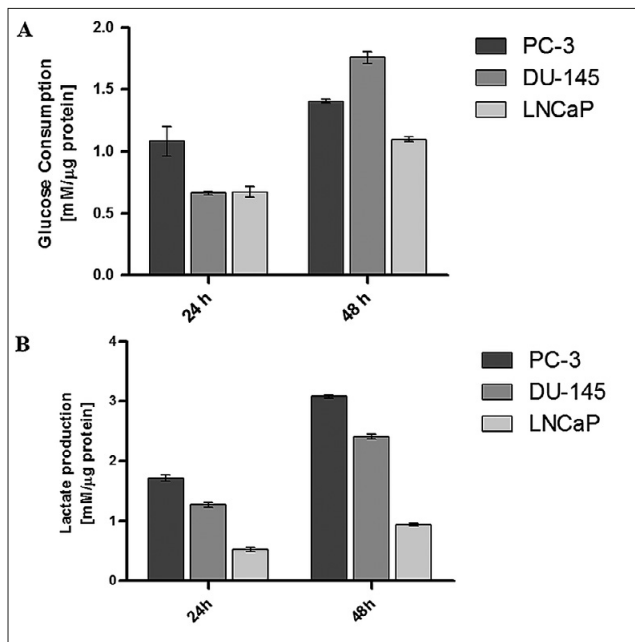


Figure 9. Changes in the concentration of **A)** glucose and **B)** lactate in the culture media of the studied cell lines during their 48-hours culturing.

The basal level of oxidative stress

Quantitative Real-Time PCR Analysis (qRT-PCR). Relative gene expression assessment revealed that in PC-3 and DU-145 cell lines genes expression related to oxidative stress were significantly lower as compared to the LNCaP cell line (Fig. 10).

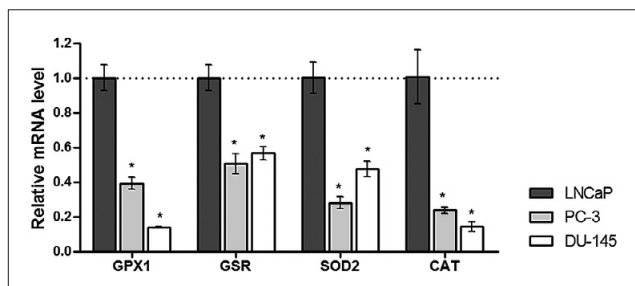


Figure 10. Relative mRNA expression level of genes related to oxidative stress. *18S RNA* and *BACT* were used as references genes. The results were calculated as RQ values and presented as the mean \pm SD value of 3 independent experiments

Reactive oxygen species (ROS) detection. The staining with CellROX Green Reagent revealed that only in a culture of LNCaP cell line fluorescence signal was observed, which implies that these cells were characterized by the highest basal ROS level, compared to other cell lines (Fig. 11).

DISCUSSION

Ionizing radiation (IR) is one of the most widely used therapeutic methods in the treatment of many types of cancer, including prostate cancer. However, due to the development of radioresistance of the tumour, it is often only a conservative treatment option. Radioresistance is a complex process by which cancer cells adapt to changes induced by IR. A growing body of evidence suggests that metabolic reprogramming in cancer is one of the major contributors to radioresistance [9]. Mitochondria play a crucial role in this process. They possess the ability to rapidly adapt to the increasing energy requirements of cancer by modulating the energy production processes in tumour cells, and radioresistance is associated with changes in the mitochondrial energy metabolism profile as well as mitochondria functions, morphology and size [14]. Therefore, one of the strategies for developing new anti-cancer therapies is to disrupt the proper functions of the mitochondria. One example of this strategy is using metformin as an anticancer drug. Some reports suggest that metformin, currently used as an antidiabetic drug, inhibits complex I of the electron transport chain, possess the ability to induce apoptosis, as well as reduce cancer cell proliferation [23, 24]. Another possibility is the uncoupling of oxidative phosphorylation.

2,4-dinitrophenol (2,4-DNP) is one of the first and thus well-described prototypical mitochondrial uncouplers that was initially introduced as a weight loss agent [25, 26]. Currently, the use of 2,4-DNP is being reconsidered in the treatment of cancer as well as metabolic and neurodegenerative diseases. The biggest challenge here is to separate the uncoupling activity of 2,4-DNP from its side-effects through physicochemical modifications, combined use of 2,4-DNP with other toxicity modifying agents, or as a prodrug [27]. Hitherto, *in vitro* studies using several human cancer cell lines, such as T-cell leukemia, lymphoblastic

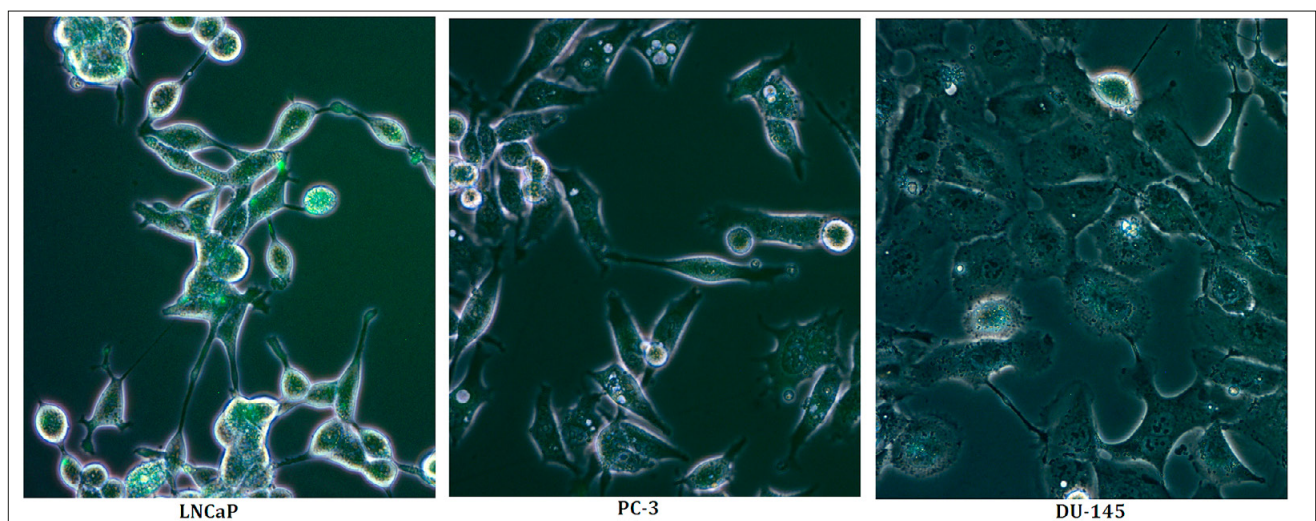


Figure 11. Basal ROS level detection using CellROX Green Reagent (magnification x 200)

leukemia, cervical cancer and pulmonary adenocarcinoma, have revealed that 2,4-DNP induces apoptosis in a dose-dependent manner, while IC_{50} was shown to be as high as 200 μ M in lung cancer cell line [25, 28, 29]. In the current study, an almost similar IC_{50} value was observed for both LNCaP and PC-3 cell lines. In the case of DU-145 cells, the IC_{50} value was 4 times higher. In further research, 2,4-DNP in 100 μ M concentration was used as a model uncoupler substance.

The main aim of the current study was to assess whether a substance that disrupts the function of mitochondria by OXPHOS uncoupling in a neoplastic cell would be able to sensitize it to IR, as well as enhance its effectiveness. Among prostate cancer cell lines used in this study, only the LNCaP cell line is androgen-sensitive (express androgen receptor) and expresses the wild-type p53. The PC-3 cell line is p53-deficient, whereas the DU-145 cell line is characterized by the presence of mutant p53. Both cell lines are androgen-insensitive and possess no functional p53. The LNCaP (androgen-sensitive) cells were much more highly sensitive to X-ray treatment, compared to other cell lines. The results are consistent with previous studies, i.e. performed by Sun et al. LNCaP cells were much more sensitive to radiation treatment than DU-145 and PC-3 cells [30, 31, 32, 33]. In addition, typical for X-ray, inhibitions of the cell cycle in the G2/M phase was observed. Zdrowowicz et al. in research performed on PC-3 cells used the same doses of X-ray and obtain similar results [34]. The conducted research showed that the LNCaP cell line was the most sensitive to 2,4-DNP itself (based on the IC_{50} value), characterized by the highest sensitivity to the applied radiation dose, and only in the case of this cell line, the synergistic effect of 2,4-DNP and X-ray was observed. There are many factors that may contribute to the higher sensitivity of the LNCaP cell line to radiation as well as 2,4-DNP treatment.

p53 is a well-known genome guardian activated as a result of e.g DNA damage (IR, UV, chemical agents), oxidative stress as well as deregulated oncogene expression. It plays an enormous role in the regulation or progression through the cell cycle, apoptosis and genomic stability. Nowadays, considerable attention is paid to p53 status as a metabolic modulator in cancer cells. p53 as the transcription factor directly regulates the expression of several hundred genes, among which there are also many relating to cell metabolism [35, 36]. It is considered that Wild-type p53, compared to the mutant type, may possess opposing effects in metabolic genes expression. Consequently, the metabolic targeted therapy may have a variable response depending on the p53 status of the cells. On the one hand, it may modulate the resistance to the treatment used, but on the other hand, may variously regulate the cancer metabolism by having an impact on senescence, apoptosis as well as autophagy of tumour cells [37]. p53 status could have a direct impact on the effect observed in our studies by inhibiting the cycle, but also indirectly by regulating the expression of metabolic genes and all the associated consequences. Thus, special attention must be paid to the interplay between p53 and cells metabolism during selection of the appropriate therapeutic cancer method.

To confirm the differences between the tested cell lines that could be significant for the observed effect, the metabolic phenotype of the tested cell lines was assessed. The LNCaP cell line, compared to the other cell lines, produced the

least lactate and consumed the least glucose during the 48-h incubation. A similar observation of increased lactate production in PC-3 and DU-145 cell lines, compared to the LNCaP cell line, was reported in 3 independently conducted studies [38, 39, 40]. In addition to the increased production of lactate, an increased expression of lactate dehydrogenase (LDH), responsible for the conversion of pyruvate to lactate, with the production of NAD^+ , was also demonstrated. Effert et al. [41] and Cutruzzola et al. [42] showed that the increase in lactate production is mainly due to glucose metabolism by glycolysis in the presence of oxygen, which was confirmed in the current study. These observations indirectly indicate that the LNCaP cell line produces energy primarily through mitochondrial respiration.

Mitochondrial respiration constitutes the most important source of ROS in the cell. In addition, studies have shown that the LNCaP cell line is characterized by the highest basal level of free radicals among the tested cell lines, which could explain its highest radiosensitivity (further increase in ROS as a result of radiation). Similar observations were noted by Lim et al. who observed that ROS level in LNCaP cells was twice as high, compared to PC-3 cells [43]. On the other hand, analysis of the gene expression related to antioxidant defence showed that this cell line is also distinguished by the greatest antioxidative potential. These observations show that the LNCaP cell line exhibits a higher threshold of oxidation-antioxidation balance.

Increased production of ROS is strongly associated with the occurrence of mutations in oncogenes and tumour suppressor genes. In turn, free radicals and oxidative damage play a key role in oncogenesis by activating signalling pathways, and thus regulating cellular proliferation, metabolism and angiogenesis, and hence, tumour progression [44]. Tumour-induced oxidative stress in adjacent cancer-associated fibroblasts alters tumour stromal microenvironment via HIF1- and NF κ B- activation, and thus the autophagic degradation of stromal caveolin-1 [45]. As a consequence of this strong dependence on ROS production, cancer cells are more susceptible to further disruption of their redox status than normal cells [46]. For this reason, it is probable that the LNCaP cell line seems to be the most sensitive to both radiation and the decoupling factor. The majority of uncouplers (including 2,4-DNP) were shown to increase ROS levels in cancer cells and often decreased antioxidant defence by lowering GSH and NADPH levels [25, 29].

The metabolic phenotype of prostate cancer may be the reason for the observed different effects of the simultaneous action of X-rays and 2,4-DNP in the studied prostate cancer cell lines. Comparable changes were observed between the PC-3 and DU-145 cell lines. The lack of a synergistic effect in these cell lines can be explained by a lower dependence of these cells on mitochondrial energy production, compared to the LNCaP cell line. Considerable evidence indicates that increased glycolysis may hinder radiotherapy of cancer cells, which in turn may be reflected in the lack of a synergistic effect in the PC-3 and DU-145 cell lines [47, 48, 49]. In the case of the LNCaP cell line, the demonstrated synergistic effect may result from the dependence of cell functioning on oxidative phosphorylation. This observation is confirmed by ATP level measurements, which revealed that this cell line is characterized by the highest basal ATP level. At the same time, the greatest decrease in ATP level due to the 2,4-DNP treatment was observed. Thus, it seems likely that this high

level of ATP is required, *inter alia*, to maintain an elevated level of antioxidant defence. Due to the limited number of reports on the use of 2,4-DNP in therapy and as a sensitizing agent, further in-depth studies are needed.

CONCLUSION

The simultaneous action of X-ray and 2,4-DNP resulted not only in the increased production of toxic ROS, but it prevented the cells from the antioxidant defence by inhibiting the synthesis of ATP. Consequently, the sensitivity of the tested cell line to X-ray and uncoupler may result from its metabolic phenotype dependent on oxidative phosphorylation.

Acknowledgements

Internal Grant for young researchers of Medical University of Lublin (PBmb10)

REFERENCES

- Weir HK, Anderson RN, Coleman King SM, et al. Heart Disease and Cancer Deaths – Trends and Projections in the United States, 1969–2020. *Prev Chronic Dis*. 2016;13:E157. doi:10.5888/pcd13.160211
- Cancer (IARC) TIA for R on. Global Cancer Observatory. Accessed April 15, 2022. <https://gco.iarc.fr/>
- Parker C, Gillissen S, Heidenreich A, Horwich A, ESMO Guidelines Committee. Cancer of the prostate: ESMO Clinical Practice Guidelines for diagnosis, treatment and follow-up. *Ann Oncol*. 2015;26 Suppl 5:v69–77. doi:10.1093/annonc/mdv222
- Bolus NE. Basic Review of Radiation Biology and Terminology. *J Nucl Med Technol*. 2017;45(4):259–264. doi:10.2967/jnmt.117.195230
- Burgio E, Piscitelli P, Migliore L. Ionizing Radiation and Human Health: Reviewing Models of Exposure and Mechanisms of Cellular Damage. An Epigenetic Perspective. *Int J Environ Res Public Health*. 2018;15(9):E1971. doi:10.3390/ijerph15091971
- Fabbrizi MR, Parsons JL. Radiotherapy and the cellular DNA damage response: current and future perspectives on head and neck cancer treatment. *Cancer Drug Resist*. 2020;3(4):775–790. doi:10.20517/cdr.2020.49
- Huang RX, Zhou PK. DNA damage response signaling pathways and targets for radiotherapy sensitization in cancer. *Sig Transduct Target Ther*. 2020;5(1):60. doi:10.1038/s41392-020-0150-x
- McCann E, O’Sullivan J, Marcone S. Targeting cancer-cell mitochondria and metabolism to improve radiotherapy response. *Transl Oncol*. 2021;14(1):100905. doi:10.1016/j.tranon.2020.100905
- Tang L, Wei F, Wu Y, et al. Role of metabolism in cancer cell radio-resistance and radiosensitization methods. *J Exp Clin Cancer Res*. 2018;37(1):87. doi:10.1186/s13046-018-0758-7
- Potter M, Newport E, Morten KJ. The Warburg effect: 80 years on. *Biochem Soc Trans*. 2016;44(5):1499–1505. doi:10.1042/BST20160094
- Liu C, Jin Y, Fan Z. The Mechanism of Warburg Effect-Induced Chemoresistance in Cancer. *Front Oncol*. 2021;11:698023. doi:10.3389/fonc.2021.698023
- DeBerardinis RJ, Chandel NS. We need to talk about the Warburg effect. *Nat Metab*. 2020;2(2):127–129. doi:10.1038/s42255-020-0172-2
- Vasan K, Werner M, Chandel NS. Mitochondrial Metabolism as a Target for Cancer Therapy. *Cell Metab*. 2020;32(3):341–352. doi:10.1016/j.cmet.2020.06.019
- Lynam-Lennon N, Maher SG, Maguire A, et al. Altered Mitochondrial Function and Energy Metabolism Is Associated with a Radioresistant Phenotype in Oesophageal Adenocarcinoma. *PLOS ONE*. 2014;9(6):e100738. doi:10.1371/journal.pone.0100738
- Priolo C, Pyne S, Rose J, et al. AKT1 and MYC induce distinctive metabolic fingerprints in human prostate cancer. *Cancer Res*. 2014;74(24):7198–7204. doi:10.1158/0008-5472.can-14-1490
- Yang L, Hou Y, Yuan J, et al. Twist promotes reprogramming of glucose metabolism in breast cancer cells through PI3K/AKT and p53 signaling pathways. *Oncotarget*. 2015;6(28):25755–25769. doi:10.18632/oncotarget.4697
- Geisler JG. 2,4 Dinitrophenol as Medicine. *Cells*. 2019;8(3):E280. doi:10.3390/cells8030280
- Rui L. New Antidiabetes Agent Targeting Both Mitochondrial Uncoupling and Pyruvate Catabolism: Two Birds With One Stone. *Diabetes*. 2019;68(12):2195–2196. doi:10.2337/dbi19-0024
- IC50 Calculator, AAT Bioquest. Accessed November 2, 2021. <https://www.aatbio.com/tools/ic50-calculator>
- Geraldo de Campos E, Fogarty M, Spinosa De Martinis B, Kerr Logan B. Analysis of 2,4-Dinitrophenol in Postmortem Blood and Urine by Gas Chromatography-Mass Spectrometry: Method Development and Validation and Report of Three Fatalities in the United States. *J Forensic Sci*. 2020;65(1):183–188. doi:10.1111/1556-4029.14154
- Kuznetsov AV, Javadov S, Sickinger S, Frotschnig S, Grimm M. H9c2 and HL-1 cells demonstrate distinct features of energy metabolism, mitochondrial function and sensitivity to hypoxia-reoxygenation. *Biochim Biophys Acta*. 2015;1853(2):276–284. doi:10.1016/j.bbamcr.2014.11.015
- Zhao Q, Sun Q, Zhou L, Liu K, Jiao K. Complex Regulation of Mitochondrial Function During Cardiac Development. *JAHA*. 2019;8(13):e012731. doi:10.1161/JAHA.119.012731
- Wheaton WW, Weinberg SE, Hamanaka RB, et al. Metformin inhibits mitochondrial complex I of cancer cells to reduce tumorigenesis. *eLife*. 2014;3:e02242. doi:10.7554/eLife.02242
- Sena P, Mancini S, Benincasa M, Mariani F, Palumbo C, Roncucci L. Metformin Induces Apoptosis and Alters Cellular Responses to Oxidative Stress in Ht29 Colon Cancer Cells: Preliminary Findings. *Int J Mol Sci*. 2018;19(5):E1478. doi:10.3390/ijms19051478
- Shrestha R, Johnson E, Byrne FL. Exploring the therapeutic potential of mitochondrial uncouplers in cancer. *Mol Metab*. 2021;51:101222. doi:10.1016/j.molmet.2021.101222
- Demine, Renard, Arnould. Mitochondrial Uncoupling: A Key Controller of Biological Processes in Physiology and Diseases. *Cells*. 2019;8(8):795. doi:10.3390/cells8080795
- Jiang H, Jin J, Duan Y, et al. Mitochondrial Uncoupling Coordinated With PDH Activation Safely Ameliorates Hyperglycemia via Promoting Glucose Oxidation. *Diabetes*. 2019;68(12):2197–2209. doi:10.2337/db19-0589
- Vier J, Gerhard M, Wagner H, Häcker G. Enhancement of death-receptor induced caspase-8-activation in the death-inducing signalling complex by uncoupling of oxidative phosphorylation. *Mol Immunol*. 2004;40(10):661–670. doi:10.1016/j.molimm.2003.09.008
- Han YH, Kim SW, Kim SH, Kim SZ, Park WH. 2,4-dinitrophenol induces G1 phase arrest and apoptosis in human pulmonary adenocarcinoma Calu-6 cells. *Toxicol In Vitro*. 2008;22(3):659–670. doi:10.1016/j.tiv.2007.12.005
- Sun Y, St Clair DK, Fang F, et al. The radiosensitization effect of parthenolide in prostate cancer cells is mediated by nuclear factor-kappaB inhibition and enhanced by the presence of PTEN. *Mol Cancer Ther*. 2007;6(9):2477–2486. doi:10.1158/1535-7163.MCT-07-0186
- van Bokhoven A, Varella-Garcia M, Korch C, et al. Molecular characterization of human prostate carcinoma cell lines. *Prostate*. 2003;57(3):205–225. doi:10.1002/pros.10290
- Josson S, Xu Y, Fang F, Dhar SK, St Clair DK, St Clair WH. RelB regulates manganese superoxide dismutase gene and resistance to ionizing radiation of prostate cancer cells. *Oncogene*. 2006;25(10):1554–1559. doi:10.1038/sj.onc.1209186
- Scott SL, Gumerlock PH, Beckett L, Li Y, Goldberg Z. Survival and cell cycle kinetics of human prostate cancer cell lines after single- and multifraction exposures to ionizing radiation. *Int J Radiat Oncol Biol Phys*. 2004;59(1):219–227. doi:10.1016/j.ijrobp.2004.01.027
- Zdrowowicz M, Datta M, Rychłowski M, Rak J. Radiosensitization of PC3 Prostate Cancer Cells by 5-Thiocyanato-2'-deoxyuridine. *Cancers*. 2022;14(8):2035. doi:10.3390/cancers14082035
- Humpton TJ, Vousden KH. Regulation of Cellular Metabolism and Hypoxia by p53. *Cold Spring Harb Perspect Med*. 2016;6(7):a026146. doi:10.1101/cshperspect.a026146
- Hafner A, Bulyk ML, Jambhekar A, Lahav G. The multiple mechanisms that regulate p53 activity and cell fate. *Nat Rev Mol Cell Biol*. 2019;20(4):199–210. doi:10.1038/s41580-019-0110-x
- Simabuco FM, Morale MG, Pavan ICB, Morelli AP, Silva FR, Tamura RE. p53 and metabolism: from mechanism to therapeutics. *Oncotarget*. 2018;9(34):23780–23823. doi:10.18632/oncotarget.25267
- Higgins LH, Withers HG, Garbens A, et al. Hypoxia and the metabolic phenotype of prostate cancer cells. *Biochim Biophys Acta*. 2009;1787(12):1433–1443. doi:10.1016/j.bbabi.2009.06.003
- Vaz CV, Alves MG, Marques R, et al. Androgen-responsive and nonresponsive prostate cancer cells present a distinct glycolytic metabolism profile. *Int J Biochem Cell Biol*. 2012;44(11):2077–2084. doi:10.1016/j.biocel.2012.08.013

40. Pertega-Gomes N, Felisbino S, Massie CE, et al. A glycolytic phenotype is associated with prostate cancer progression and aggressiveness: a role for monocarboxylate transporters as metabolic targets for therapy. *J Pathol.* 2015;236(4):517–530. doi:10.1002/path.4547
41. Effert P, Beniers AJ, Tamimi Y, Handt S, Jakse G. Expression of glucose transporter 1 (Glut-1) in cell lines and clinical specimens from human prostate adenocarcinoma. *Anticancer Res.* 2004;24(5A):3057–3063.
42. Cutruzzolà F, Giardina G, Marani M, et al. Glucose Metabolism in the Progression of Prostate Cancer. *Front Physiol.* 2017;8:97. doi:10.3389/fphys.2017.00097
43. Lim HW, Hong S, Jin W, et al. Up-regulation of defense enzymes is responsible for low reactive oxygen species in malignant prostate cancer cells. *Exp Mol Med.* 2005;37(5):497–506. doi:10.1038/emm.2005.62
44. Sullivan LB, Chandel NS. Mitochondrial reactive oxygen species and cancer. *Cancer Metab.* 2014;2(1):17. doi:10.1186/2049–3002–2–17
45. Martinez-Outschoorn UE, Trimmer C, Lin Z, et al. Autophagy in cancer associated fibroblasts promotes tumor cell survival: Role of hypoxia, HIF1 induction and NFκB activation in the tumor stromal microenvironment. *Cell Cycle.* 2010;9(17):3515–3533. doi:10.4161/cc.9.17.12928
46. Sznarkowska A, Kostecka A, Meller K, Bielawski KP. Inhibition of cancer antioxidant defense by natural compounds. *Oncotarget.* 2017;8(9):15996–16016. doi:10.18632/oncotarget.13723
47. Bing Z, Yang G, Zhang Y, et al. Proteomic analysis of effects by x-rays and heavy ion in HeLa cells. *Radiology and Oncology.* 2014;48(2):142–154. doi:10.2478/raon-2013–0087
48. van Gisbergen MW, Zwilling E, Dubois LJ. Metabolic Rewiring in Radiation Oncology Toward Improving the Therapeutic Ratio. *Front Oncol.* 2021;11:653621. doi:10.3389/fonc.2021.653621
49. Nile DL, Rae C, Walker DJ, et al. Inhibition of glycolysis and mitochondrial respiration promotes radiosensitisation of neuroblastoma and glioma cells. *Cancer Metab.* 2021;9(1):24. doi:10.1186/s40170–021–00258–5